UC Santa Barbara
UC Santa Barbara Previously Published Works

Title
Si doping effect on strain reduction in compressively strained Al0.49Ga0.51N thin films

Permalink
https://escholarship.org/uc/item/0h8913hd

Journal
Applied Physics Letters, 83(4)

ISSN
0003-6951

Authors
Cantu, P
Wu, F
Waltereit, P
et al.

Publication Date
2003-07-01

Peer reviewed

eScholarship.org Powered by the California Digital Library
University of California

Si doping effect on strain reduction in compressively strained $Al_{0.49}Ga_{0.51}N$ thin films

P. Cantu,[a] F. Wu, P. Waltereit, S. Keller, A. E. Romanov,[b] U. K. Mishra, S. P. DenBaars, and J. S. Speck
Electrical and Computer Engineering Department and Materials Department, University of California Santa Barbara, Santa Barbara, California 93106

(Received 28 February 2003; accepted 5 June 2003)

Evaluation of the structural properties of 200-nm-thick Si-doped $Al_{0.49}Ga_{0.51}N$ films, grown on nominally relaxed 1-μm-thick $Al_{0.62}Ga_{0.38}N$ buffer layers on sapphire, revealed that increased Si doping promoted the relaxation of the compressively strained layers. The degree of strain relaxation R of the $Al_{0.49}Ga_{0.51}N$ films, as determined by x-ray diffraction (XRD), increased from $R=0.55$ to $R=0.94$ with an increase in disilane injection from 1.25 nmol/min to 8.57 nmol/min. Transmission electron microscopy analysis showed that the edge threading dislocations (TDs) in the $Al_{0.49}Ga_{0.51}N$ layers were inclined, such that the redirected TD lines had a misfit dislocation component. The calculated strain relaxation due to the inclined TDs was in close agreement with the values determined from XRD. We propose that the TD line redirection was promoted by the Si-induced surface roughness. © *2003 American Institute of Physics.* [DOI: 10.1063/1.1595133]

Low-resistivity, n-type, high-AlN-mole-fraction (x) $Al_xGa_{1-x}N$ alloys are necessary for the fabrication of deep ultraviolet optoelectronic devices. However, growth of this alloy becomes more difficult with increasing x. In general, $Al_xGa_{1-x}N$ films with $x \geqslant 0.20$ deposited directly on c-plane sapphire substrates exhibit threading dislocation (TD) densities in the $10^{10}-10^{11}\ cm^{-2}$ range,[1] in comparison to $10^8-10^9\ cm^{-2}$ for GaN. The higher TD density is related to the low surface mobility of the Al species during deposition, which prevents the formation of large islands in the initial stage of growth. Additionally, growth of $Al_xGa_{1-x}N$ films on nominally relaxed $Al_yGa_{1-y}N$ buffers results in either tensile ($x>y$) or compressive ($x<y$) biaxial stresses. Doping high-Al-composition AlGaN films is also a challenge. Even though the n-type dopant Si is readily incorporated in $Al_xGa_{1-x}N$ films, its electrical activity decreases with increasing x.[2] At Al mole fractions exceeding 0.50, the Si donor level was reported to transform into a deep level, related to the formation of a DX center.[3] Furthermore, the doping efficiencies are affected by self-compensation processes. For example, the probability to form gallium and aluminum vacancies, which possess acceptor character, strongly increases with increasing x in n-type $Al_xGa_{1-x}N$ films.[4]

In this letter, we report on the effect of Si doping on the structural properties of 200-nm-thick $Al_{0.49}Ga_{0.51}N$ films deposited on top of 1-μm-thick $Al_{0.62}Ga_{0.38}N$ buffer layers on sapphire. The $Al_{0.49}Ga_{0.51}N$ films had a nominal misfit strain of approximately 0.32% with respect to the $Al_{0.62}Ga_{0.38}N$ buffer layers. It was observed that increased Si doping enhanced the strain relaxation of the $Al_{0.49}Ga_{0.51}N$ films by edge TD line redirection.

All samples were grown by low-pressure metalorganic chemical vapor deposition (MOCVD) at 100 Torr, on c-plane sapphire substrates using trimethylgallium (TMG), trimethylaluminum (TMA), and ammonia (NH_3) as precursors. Disilane ($DiSi=Si_2H_6$) was introduced into the gas stream to achieve Si doping.

The growth of all samples was initiated with the deposition of a 14-nm-thick $Al_{0.60}Ga_{0.40}N$ nucleation layer at 600 °C. Next, the temperature was raised to 1150 °C to deposit a 1-μm-thick $Al_{0.62}Ga_{0.38}N$ buffer layer using TMG and TMA flows of 29.5 μmol/min and 35.5 μmol/min, respectively. H_2 was used as carrier gas. Next, 200-nm-thick Si-doped $Al_{0.49}Ga_{0.51}N$ films were deposited on top of the buffer layers also at 1150 °C, using TMG and TMA flows of 10.5 μmol/min and 7.1 μmol/min, respectively. The DiSi flow rate during growth was varied between 1.25 and 8.57 nmol/min, which resulted in silicon incorporations of $[Si]=1.42\times10^{19}\ cm^{-3}$ and $[Si]=9.72\times10^{19}\ cm^{-3}$, respectively, as calculated from secondary ion mass spectroscopy data taken from doping calibration samples grown under similar conditions. N_2 was used as carrier gas. A constant NH_3 flow of 45 mmol/min was used for both the buffer and doped layers.

The structural properties were evaluated by high-resolution x-ray diffraction (XRD) measurements, conducted on a Philips Materials Research Diffractometer. Atomic force microscopy (AFM) was performed using a Digital Instruments Nanoscope III operated in tapping mode. The rms roughness values were obtained using the computer software. Transmission electron microscopy (TEM) was carried out using a JEOL 2000FX.

Several $Al_{0.49}Ga_{0.51}N$ samples were grown with different Si injections to optimize the n-type doping in the films. For these type of samples, we routinely determined the Al composition by measuring $2\theta-\omega$ XRD scans in the symmetric (0002) and (0004) reflections, using a receiving slit. Surprisingly, we observed a shift of the relative position of the $Al_{0.49}Ga_{0.51}N$ (000l) peak with respect to the $Al_{0.62}Ga_{0.38}N$ (000l) peak for samples grown with different DiSi injections. The measured peak separation between the

[a]Electronic mail: pcantu@engineering.ucsb.edu
[b]Permanent Address: A.F. Ioffe Physico-Technical Institute, 194021 St. Petersburg, Russia.

 © 2003 American Institute of Physics
Downloaded 22 Jul 2003 to 128.111.74.212. Redistribution subject to AIP license or copyright, see http://ojps.aip.org/aplo/aplcr.jsp

$Al_{0.62}Ga_{0.38}N$ and $Al_{0.49}Ga_{0.51}N$ $(000l)$ reflections decreased with increasing Si doping, indicating that either the composition or the strain in the $Al_{0.49}Ga_{0.51}N$ layers was changing (the run-to-run variation in the layer composition for undoped samples was less than 1% in our reactor). However, as the symmetric scans were not capable of determining both the composition and the strain state of the $Al_{0.49}Ga_{0.51}N$ layers, thus we used reciprocal space maps (RSMs) near the $(10\bar{1}5)$ asymmetric reflection to unambiguously determine strain and composition.

We measured XRD RSMs near the $(10\bar{1}5)$ reflection, taken in coplanar geometry (incident and scattered wave vectors and sample surface normal all in the same plane) with shallow incidence of the x-ray beam, in rocking curve mode with a 1.0 mm slit. For these maps, the $(1,1,\bar{2},12)$ reflection of sapphire ($a = 0.47588$ nm and $c = 1.2992$ nm) was employed as an angular reference at $\theta_0 = 51.412°$ (Bragg angle) and $\omega_0 = 26.946°$ (reference incidence angle between the incident beam and the $(000l)$ planes). Using the known sapphire lattice constants, the in-plane and out-of-plane cell dimensions of the 1-μm-thick $Al_yGa_{1-y}N$ buffer layer were calculated from θ and ω. We then used standard x-ray analysis to determine the Al composition of the buffer layer resulting in an Al mole fraction of approximately 0.62. The degree of strain relaxation,[5] $R = 1 - \varepsilon^{\text{measured}}/\varepsilon^{\text{coherent}}$ (where $\varepsilon^{\text{measured}}$ is the actual strain in the epilayer and $\varepsilon^{\text{coherent}}$ is the strain in a coherent layer), was used as a measure of the strain state of the epilayer. The buffer layer exhibited $R \approx 0.98$ with respect to the underlying sapphire substrate. This value corresponded to a residual compressive strain of approximately 0.27%, given the lattice mismatch of $\sim 13.4\%$ between the $Al_{0.62}Ga_{0.38}N$ buffer and the sapphire substrate. The residual strain state of the $Al_{0.62}Ga_{0.38}N$ buffer was due to both the strains associated to the growth process and the compressive thermal mismatch strain during cooling to room temperature;[6] the latter was on the order of 0.30%. Thus, it is reasonable to assume that the residual strain of the $Al_{0.62}Ga_{0.38}N$ buffer at growth temperature was negligible.

The same method as just described was used to determine the cell dimensions of the $Al_{0.49}Ga_{0.51}N$ films. Figure 1(a) is a characteristic RSM that shows that the $Al_{0.49}Ga_{0.51}N$ layer was not coherent with respect to the underlying $Al_{0.62}Ga_{0.38}N$ buffer. The XRD analysis revealed that the 200-nm-thick $Al_{0.49}Ga_{0.51}N$ films were only partially relaxed with respect to the $Al_{0.62}Ga_{0.38}N$ buffer layers, and that the relaxation was the more pronounced the higher the Si doping. As shown in Fig. 1(b), we observed an increase from $R = 0.55$ to $R = 0.94$ (for the $Al_{0.49}Ga_{0.51}N$ layer with respect to the $Al_{0.62}Ga_{0.38}N$ buffer) for a corresponding increase in the Si/(Al+Ga) ratio [$2\times$DiSi flow/(TMG flow +TMA flow)] from 7.1×10^{-5} to 4.9×10^{-4}.

The reproducibility of the strain relaxation results was confirmed through several experiments conducted before and after this study, for which the XRD determined compositions of several $Al_{0.62}Ga_{0.38}N$ buffers and $Al_{0.49}Ga_{0.51}N$ films did not change more than $\pm1\%$. Hall effect measurements on Si-doped samples grown under identical conditions showed that the n-type doping level was also stable.[7] Furthermore, enhanced strain relaxation by increased Si doping was also observed for AlGaN/AlGaN strained layer superlattices, which were grown on similar $Al_{0.62}Ga_{0.38}N$ buffer layers.[8]

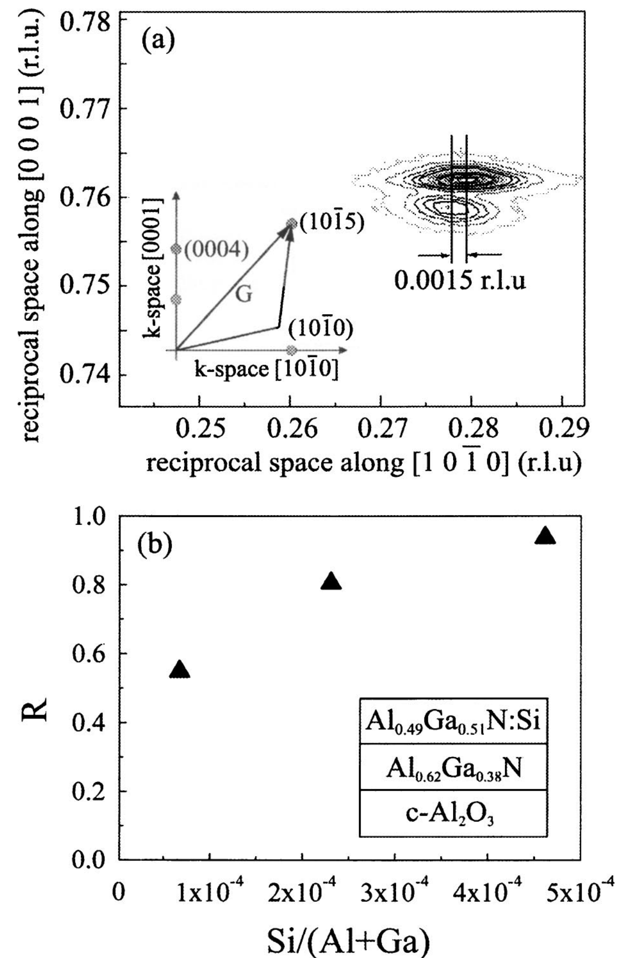

FIG. 1. (a) RSM near the asymmetric $(10\bar{1}5)$ reflection of the epilayer stack. The map was taken in coplanar geometry with shallow incidence and rocking curve configuration. "r.l.u" refers to dimensionless reciprocal lattice units (λq). (b) Degree of strain relaxation of Si-doped $Al_{0.49}Ga_{0.51}N$ films as obtained from x-ray analysis of RSMs. The inset is a schematic of the sample structures.

In the growth of GaN, silicon has been established as an antisurfactant and similar roughening effects were observed in high-Al-content AlGaN layers.[9,10] Figures 2(a) and 2(b) show AFM images of $Al_{0.49}Ga_{0.51}N$ films grown with Si/(Al+Ga) ratios of 7.1×10^{-5} and 4.9×10^{-4}, respectively. The measured rms roughness over the 1-μm $\times$1-μm scans increased from 0.32 nm for Fig. 2(a), to 0.80 nm for Fig. 2(b). Si doping enhanced the formation of small

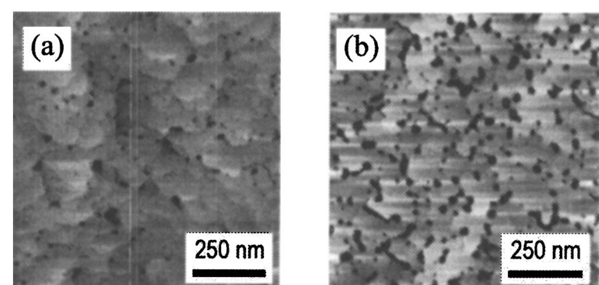

FIG. 2. AFM images of $Al_{0.49}Ga_{0.51}N$ films doped with (a) Si/(Al+Ga) $=7.1\times10^{-5}$ and (b) Si/(Al+Ga)$=4.9\times10^{-4}$. The rms surface roughness values measured from the 1-μm$\times$1-μm images were (a) 0.32 nm and (b) 0.80 nm.

Downloaded 22 Jul 2003 to 128.111.74.212. Redistribution subject to AIP license or copyright, see http://ojps.aip.org/aplo/aplcr.jsp

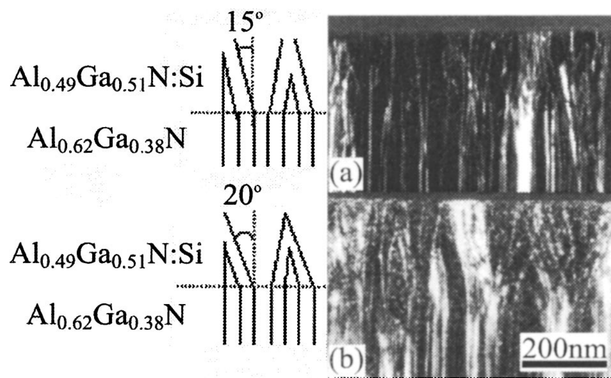

FIG. 3. Cross-sectional TEM images of $Al_{0.49}Ga_{0.51}N/Al_{0.62}Ga_{0.38}N$ single heterostructures, where (a) and (b) are $11\bar{2}0$ weak-beam, dark-field images of the samples doped with Si/(Al+Ga) ratios of 7.1×10^{-5} and 4.9×10^{-4}, respectively. The measured angles of (a) 15° and (b) 20° were a 30° projection of the real inclination angles, which were (a) 17.2° and (b) 22.8°.

pits at the intersection of dislocations with the sample surface, as seen for the sample grown with the highest Si/(Al+Ga) ratio of 4.9×10^{-4} in Fig. 2(b).

TEM analysis showed that more than 90% of the threading dislocations in our samples had Burgers vector $\frac{1}{3}\langle 11\bar{2}0\rangle$. The TD density of an $Al_{0.62}Ga_{0.38}N$ buffer grown under identical conditions was $\sim3\times10^{10}$ cm^{-2} (from plan-view TEM measurements). In the buffer, the TDs had a [0001] line direction and did not provide any strain relief. In the $Al_{0.49}Ga_{0.51}N$ cap layer, however, the TDs were inclined by $\sim10°-25°$, as seen on cross-sectional TEM images in Fig. 3. Plan-view TEM studies on similar samples showed that the TDs inclined toward the $\langle 1\bar{1}00\rangle$ directions and had a misfit component, thus relieving misfit strain (e.g., TDs with $b=\pm\frac{1}{3}[2\bar{1}\bar{1}0]$ were inclined towards $\pm[01\bar{1}0]$). The misfit component of the TDs in this geometry was obtained from the projected length of the TDs on the (0001) plane. The total biaxial plastic strain relaxation at the top layer surface caused by the inclined TDs was obtained from $\varepsilon_{\rm pl}^{\rm top}=\frac{1}{2}bL\rho$, where b is the magnitude of the edge misfit component of the Burgers vector, L the average misfit segment length, and ρ the TD density. We noted that the inclined TDs led, in an approximation, to a linear gradient in relieved strain. Figures 3(a) and 3(b) show $11\bar{2}0$ weak-beam cross-sectional TEM images of samples in which the $Al_{0.49}Ga_{0.51}N$ layers were grown with Si/(Al+Ga) ratios of 7.1×10^{-5} and 4.9×10^{-4}, respectively. The measured angles of inclination in the figures are 15° for Fig. 3(a) and 20° for Fig. 3(b), and correspond to true inclination angles of 17.2° and 22.8°, respectively, after accounting for geometric projection. For the $Al_{0.49}Ga_{0.51}N$ sample grown with the low Si/(Al+Ga) ratio of 7.1×10^{-5}, the average projected misfit dislocation segment length was 62 nm, which led to a calculated relaxed strain at the surface of 0.27% ($R=0.84$). For the $Al_{0.49}Ga_{0.51}N$ sample grown with the high Si/(Al+Ga) ratio of 4.9×10^{-4}, the average projected misfit segment length of the inclined TDs was 84 nm and the calculated relaxed strain was 0.35% ($R=1.09$) of the misfit strain at the surface. We believe that this was in good agreement with the XRD results already reported.

As shown above that the inclined TDs contributed to the misfit stress relaxation of the $Al_{0.49}Ga_{0.51}N$ films with respect to the underlying $Al_{0.62}Ga_{0.38}N$ buffer layers. We assumed that the mechanism responsible for the inclination of TDs is not a dislocation glide process. In general, for planar (0001)-oriented nitride samples with hexagonal crystal structure, the majority of the TDs have pure edge character, with [0001] line direction and Burgers vector in the basal plane. The $\{1\bar{1}00\}$ prismatic glide planes of these edge dislocations are normal to the biaxial stress plane and are free of shear stress. Thus, there is no easy slip system for plastic relaxation via dislocation glide. We propose that the observed surface roughness of the $Al_{0.49}Ga_{0.51}N$ films assisted during the initial stage of TD line redirection. The TD lines inclined at one point during growth, and maintained their new orientation throughout the growing film. Hence, we concluded that bulk diffusion-assisted climb processes were unnecessary to realize these dislocation geometries. Rather, a possible mechanism can be described as directional migration and incorporation of adatoms in the pre-existing dislocation configurations at the growing film surface. A model explaining stress-driven TD inclination will be presented elsewhere.[11] We suppose that the inclination angle was determined by the MOCVD growth conditions responsible for the surface roughness of the growing film (Si injection, growth rate, temperature, etc.). Experiments are under way to clarify the important parameters that determine the TD line orientation.

In summary, increased Si doping enhanced the relaxation of compressively strained 200-nm-thick $Al_{0.49}Ga_{0.51}N$ films grown on top of 1-μm-thick $Al_{0.62}Ga_{0.38}N$ buffer layers. The degree of relaxation obtained from XRD RSMs and TEM analysis were in good agreement. Strain relaxation was achieved by the inclination of pure edge threading dislocation lines with respect to the surface normal. The redirection of TD lines was induced by surface roughness during growth.

The authors gratefully acknowledge the support of DARPA through contracts under direction of Dr. Edgar Martinez and LTC Dr. John Carrano.

[1] M. Iwaya, S. Terao, N. Hayashi, T. Kashima, H. Amano, and I. Akasaki, Appl. Surf. Sci. **159–160**, 405 (2000).
[2] A. Y. Polyakov, N. B. Smirnov, A. V. Govorkov, M. G. Milividskii, J. M. Redwing, M. Shin, M. Skowronski, D. W. Greve, and R. G. Wilson, Solid-State Electron. **42**, 627 (1998).
[3] C. Skierbiszewski, T. Suski, M. Leszczynski, M. Shin, M. Skowronski, M. D. Bremser, and R. F. Davis, Appl. Phys. Lett. **74**, 3833 (1999).
[4] C. Stampfl and C. G. Van de Walle, Appl. Phys. Lett. **72**, 459 (1998).
[5] O. Brandt, P. Waltereit, and K. H. Ploog, J. Phys. D **35**, 577 (2002).
[6] T. Bottcher, S. Einfeldt, S. Figge, R. Chierchia, H. Heinke, D. Hommel, and J. S. Speck, Appl. Phys. Lett. **78**, 1976 (2001).
[7] P. Cantu, S. Keller, U. K. Mishra, and S. P. DenBaars, Appl. Phys. Lett. **82**, 3683 (2003).
[8] S. Keller, P. Waltereit, P. Cantu, U. K. Mishra, J. S. Speck, and S. P. DenBaars, Opt. Mater. (Amsterdam, Neth.) **23**, 187 (2003).
[9] S. Keller, U. K. Mishra, S. P. DenBaars, and W. Seifert, Jpn. J. Appl. Phys. **37**, L431 (1998).
[10] A. Munkholm, C. Thompson, M. V. Ramana Murty, J. A. Eastman, O. Auciello, G. B. Stephenson, P. Fini, S. P. DenBaars, and J. S. Speck, Appl. Phys. Lett. **77**, 1626 (2000).
[11] J. S. Speck and A. E. Romanov (unpublished).

Downloaded 22 Jul 2003 to 128.111.74.212. Redistribution subject to AIP license or copyright, see http://ojps.aip.org/aplo/aplcr.jsp